ISBN: 978-3-95450-132-8 doi:10.18429/JACoW-IPAC2014-MOPRI101

FIELD SIMULATIONS AND MECHANICAL IMPLEMENTATION OF ELECTROSTATIC ELEMENTS FOR THE ELENA TRANSFER LINES

D. Barna*, University of Tokyo, Japan
W. Bartmann, J. Borburgh, C. Carli, G. Vanbavinckhove, CERN, Geneva, Switzerland

Abstract

The Antiproton Decelerator (AD) complex at CERN will be extended by an extra low energy anti-proton ring (ELENA) [1] further decelerating the anti-protons thus improving their trapping. The kinetic energy of 100 keV at ELENA extraction facilitates the use of electrostatic transfer lines to the experiments. The mechanical implementation of the electrostatic devices are presented with focus on their alignment, bakeout compatibility, ultra-high vacuum compatibility and polarity switching. Field optimisations for an electrostatic crossing device of three beam lines are shown.

INTRODUCTION

At low particle energies electrostatic beamline elements have many advantages over magnetic ones, such as absence of remanent magnetic fields, no need for cooling, cheap production, etc. In contrast to magnets, these devices must be mounted within the beam pipes. They need to comply with the following requirements:

- Compatibility with the high vacuum required in the beamlines: 10^{-11} mbar
- Bakeability at 250 C
- Have a mechanical aperture of 60 mm, adopted for all beam line elements

Figure 1 shows the schematic layout of the transfer lines, which was constrained by the position of the existing experiments, concrete shieldings and other installation already present in the experimental hall. Devices indicated as *Fast switch + bend* will be able to separate and distribute the 4 subsequent bunches (~1 μs spacing) of one deceleration cycle to different experiments. More details about the beamline layout and optics can be found on the project webpage [2].

ELECTROSTATIC DEVICES

Ion Switch

A dedicated ion source will provide H- ions or protons for the commissioning of the ELENA ring while the experiments are still using the 5.3 MeV antiproton beam delivered by the AD. An electrostatic switchyard (ion switch) will be located at the intersection of the lines LNS, LNI and LNE00. It will either deflect protons and H- ions by 43° into the injection line LNE (with inverted polarity of the ring for protons), or protons by 43° in the reverse direction (LNE00) with normal polarity of the ring. H- ions (injected via LNI into ELENA and ejected through LNE00) can later be used to commission and tune the transfer lines even between antiproton bunches from the AD. The device must act as an undisturbed drift space for particles ejected from the AD into ELENA, or ejected from ELENA to the transfer lines.

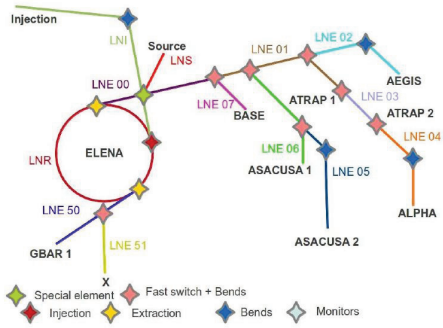

Figure 1: Schematic layout of the ELENA transfer lines.

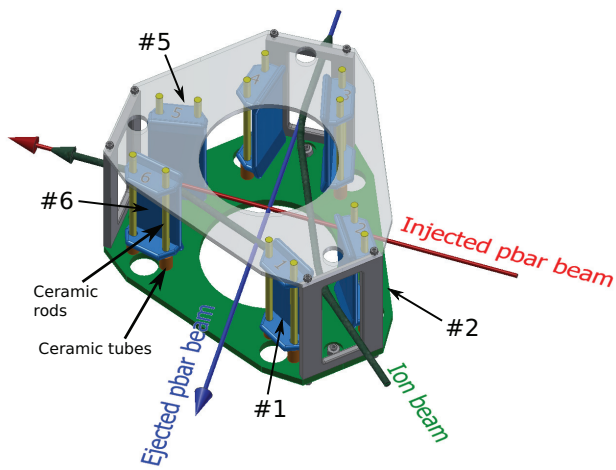

Figure 2: The electrode structure of the ion switch.

Figure 2 shows the electrode structure of the ion switch, which will be housed in a vacuum tank of diameter 450 mm. The electrodes are supported by two vertical ceramic rods and tubes, which are just dropped into the precise support frame. One of the holes on the electrodes has a racetrack shape - this design allows the different thermal expansion of the structure during bakeout in both horizontal and vertical directions, without compromising alignment precision.

The arrangement of the electrodes was chosen such that the active electrodes of an operating mode are symmetric between the input/output trajectories of the deflected ions (for example electrodes 5 and 6 are the mirror images of electrodes 2 and 1, respectively, with respect to the midplane between input and left output). This symmet-

* daniel.barna@cern.ch

ISBN: 978-3-95450-132-8 doi:10.18429/JACoW-IPAC2014-MOPRI101

ric arrangement ensures that for any voltage combination ($U_{attractive}$,$U_{repulsive}$) giving the required deflection of 43° the output beam will have zero displacement from the nominal position.

The different operating modes of the device (H- ions or protons, normal or inverse injection into the ring) will be realized by different biasing of the electrodes using high-voltage switches. The nominal voltage of the electrodes is ±26.2 kV. Figure 3 shows simulated particle trajectories in the device. The beam center has a distance of at least 30 mm from the electrodes everywhere.

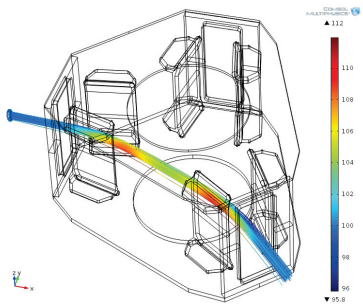

Figure 3: Simulated trajectories of the ion switch.

Electrostatic Quadrupole and Corrector Module

The beam optics of the transfer lines uses two functional classes of quadrupoles:

- Single quadrupoles with a repetition period of 1.5 m will constitute the FODO structures
- Doublets are used to re-match the beam to the FODO structures after the strongly focusing spherical deflectors

In order to facilitate design, manufacturing and spare part management, a single standard module will be used at all locations, which contains two quadrupoles and a corrector at its centre, as shown in Fig. 4. In case the unit is used in a FODO structure, only one quadrupole will be connected to a power supply. This gives also a redundancy to use the other quadrupole in case of an electrical connection problem inside the vacuum chamber.

The electrodes of the quadrupoles are extruded aluminium profiles cut to 100 mm length. All electrodes are mounted on longitudinal support rails, which are fixed to a circular disk on one end, and have a sliding support on their other end to allow thermal expansion during bakeout. The aperture disks between quadrupoles and corrector limit the electric field of each unit and render the structure more rigid.

The nominal voltage of the FODO quadrupoles is ±811 V which gives 90° phase advance per cell. The maximum voltage of the matching quadrupoles is ±5 kV. The maximum voltage of the correctors is ±1.5 kV which gives 10 mm displacement of the beam over 1.5 m (the period of the FODO structure).

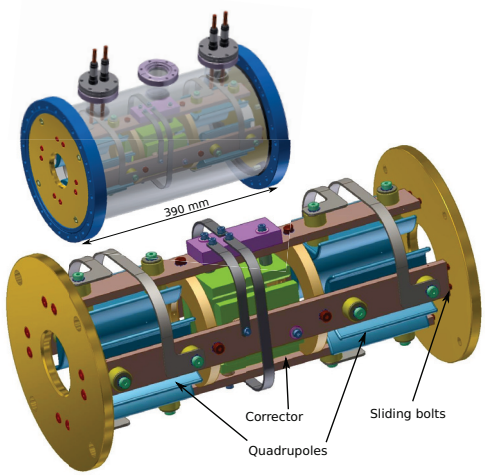

Figure 4: The quadrupole+corrector unit.

In order to test whether any nonlinearities occur at the highest voltage settings, two sets of parallel input trajectories at different input coordinates (-22 mm< x_{in} <22 mm, y_{in} = 0) and (x_{in} = 0, -22 mm< y_{in} <22 mm) were traced through the device (in a region ±120 mm around the center of the quadrupole, in order to account for the fringe fields) at a voltage of ±5 kV. Figure 5 shows the output phase-space coordinates (x'_{out},x_{out}) and (y'_{out},y_{out}) of these particles.

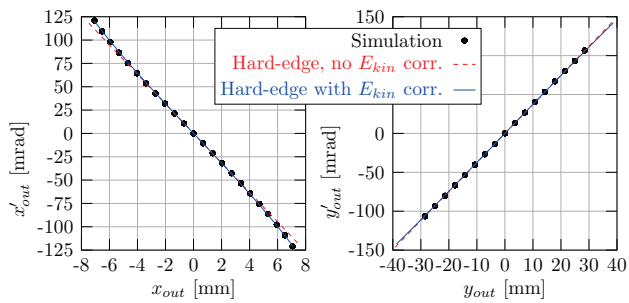

Figure 5: Output phase-space coordinates of simulated trajectories in the quadrupole at ±5 kV.

A hard-edge quadrupole model with the same voltage and an effective electrode length of 108 mm describes very well the simulated points in the full range in the defocusing plane, and around the center in the focusing plane. However, there is a slight deviation from this linear model in the focusing plane for larger coordinates. This can be very well described (solid blue line in Fig. 5) by a kinetic energy correction of the hard-edge model, by replacing the spatial oscillation frequency of the particles $\omega_z = \sqrt{|qV_0|/r_0^2 E_{kin}} \rightarrow \sqrt{|qV_0|/(r_0^2 E_{kin} - qV_0(y^2 - x^2))}$ in the transfer matrices:

$$\underset{\text{Focusing plane}}{\begin{pmatrix} \cos(\omega_z L) & \sin(\omega_z L)/\omega_z \\ -\sin(\omega_z L)\omega_z & \cos(\omega_z L) \end{pmatrix}} \underset{\text{Defocusing plane}}{\begin{pmatrix} \cosh(\omega_z L) & \sinh(\omega_z L)/\omega_z \\ \sinh(\omega_z L)\omega_z & \cosh(\omega_z L) \end{pmatrix}} \quad (1)$$

where $\pm V_0$ is the voltage applied to the electrodes, r_0 is the radius of the inscribed circle between the electrodes and q is

ISBN: 978-3-95450-132-8 doi:10.18429/JACoW-IPAC2014-MOPRI101

the particle's charge. This correction accounts for the kinetic energy change (and therefore the shorter/longer travel time) of off-axis particles. The observed nonlinearity is small and since the particles pass through typically no more than one or two such strong quadrupoles, it will not lead to beam size blow-up.

Polarity switching of the quadrupoles is a major change to the beamline optics which will not occur regularly. If needed, this can be realized by swapping the high-voltage cables at the connectors. On the other hand, polarity switching of the correctors is part of the everyday routine of beam steering. A pair of opposite corrector electrodes will be powered by two unipolar power supplies of opposite polarity. Polarity switching will be realized by high-voltage switches. This configuration constitutes a non-negligible reduction in price compared to two bipolar power supplies.

Deflectors

Spherical deflectors consisting of two concentric spherical electrodes will be used to deflect the beam in the beamlines. Constraints on the beamline layout did not allow to have a unique deflection angle at all locations. Fortunately these angles differ only by a few degrees. To facilitate design, manufacturing and spare parts management, standardized devices will be used with slightly different voltage settings (around ~ ±11.5 kV). The deflectors of the beamlines can be categorized into the following groups.

- At those locations where quick switching is not needed, a standalone spherical deflector with an angle of 47.84° will be used to realize bending angles between 46.12° and 49.56°
- Quick switching will be realized by a combination of a static spherical deflector with a fast (switching time <1 μs) electrostatic deflector (the same device that is used to eject the beam from ELENA). The fast deflector gives an initial deflection of 220 mrad to the beam.
  - A horizontal spherical deflector of 34.37° will provide a total deflection between ~46-48°
  - A vertical spherical deflector of 77.4° will bend the beam to the two vertical experiments ATRAP1 and ATRAP2.

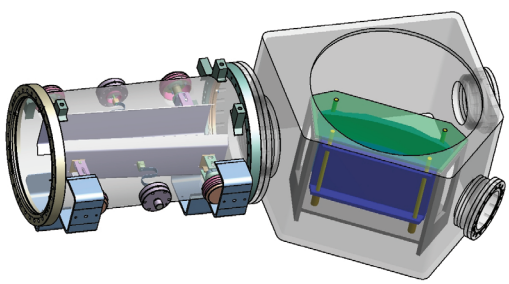

Figure 6: Horizontal quick switch combination.

Figure 6 shows the horizontal quick switch combination. The electrodes are supported using the same principle as explained above for the ion switch. A 400 mm CF flange on top of the vacuum chamber provides access to introduce and mount the electrodes and their support frame into the vacuum tank. A metal plate fixed to the back plane of the support frame of the electrodes shields the non-deflected beam from the electric field of the electrodes.

HIGH-VOLTAGE FEEDTHROUGHS AND CONTACTS

The high-voltage bias of the electrodes will be provided by vacuum feedthroughs. Since all of these devices operate under static conditions, the electrodes will not draw high currents, and the quality of the electrical contacts is not critical. Electrical contact between the electrodes and the pins of the feedthroughs will be realized using spring-loaded elements which allow the moving/expansion of different parts during bakeout, and make it possible to mount or dismantle the feedthroughs and the electrodes independently from each other (fig. 7). The material of the springs was chosen to be Nivaflex since this alloy keeps its elastic properties up to 350 C and is commonly used in micromechanics.

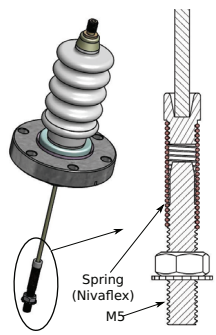

Figure 7: Principle of the spring-loaded electrical contacts.

CONCLUSIONS

The ELENA transfer lines will use electrostatic elements to deliver the antiproton beam to the experiments. A switchyard will inject H- ions and protons into the ring for commissioning. Subsequent bunches of one extraction will be distributed to different experiments using a combination of a fast deflector and a static spherical electrostatic deflector. A standard unit of two quadrupoles with 100 mm long electrodes and a corrector will be used to focus and steer the beam. The behaviour of the quadrupoles can be well described by a hard-edge model of an effective length of 108 mm with a position-dependent energy correction up to the maximum voltage of ±5 kV.

REFERENCES

[1] V. Chohan (editor) et al., "Extra Low ENergy Antiproton (ELENA) ring and its Transfer Lines: Design Report", http://cds.cern.ch/record/1694484

[2] http://cern.ch/project-elena-optics